



Thermodynamic study and electrochemical Investigation of 4-chloro-1H-pyrazolo[3,4-d]pyrimidine as a corrosion Inhibitor for mild steel in hydrochloric acid Solution

R. Chami¹, M. Boudalia², S. Echihi^{2,3}, M. El Fal^{4,5}, A. Bellaouchou²,
A. Guenbour², M. Tabyaoui², E.M. Essassi⁴, A. Zarrouk⁶, Y. Ramli⁵

¹ *Laboratoire de Physico-Chimie des Matériaux Inorganiques et Organiques, Ecole Normale Supérieure, Université Mohammed V, Rabat, Morocco*

² *Laboratory of Materials, Nanotechnology and Environment, Faculty of Sciences, University of Mohammed V. Av. Ibn Battouta, BP 1014, Rabat, Morocco.*

³ *Laboratory of Water and Environment, Faculty of Sciences, El jadida, BP 20, 24000 El jadida, Morocco*

⁴ *Laboratoire de Chimie Organique Hétérocyclique URAC 21, Pôle de Compétence Pharmacochimie, Av. Ibn Battouta, BP 1014, Faculté des Sciences, Université Mohammed V, Rabat, Morocco,*

⁵ *Medicinal Chemistry Laboratory, Faculty of Medicine and Pharmacy, Mohammed V University, Rabat, Morocco.*

⁶ *LC2AME-URAC 18, Faculty of Science, First Mohammed University, PO Box 717, 60 000 Oujda, Morocco.*

Received 16 May 2016,

Revised 31 July 2017,

Accepted 03 Aug 2017,

Keywords

- ✓ pyrimidine derivatives,
- ✓ Steel,
- ✓ Corrosion inhibition,
- ✓ Polarization curves,
- ✓ EIS.

rajaechimie@yahoo.fr,
maria.boudalia@yahoo.fr

Abstract

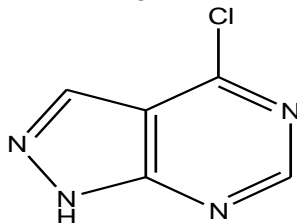
The corrosion performance of mild steel in 1 M HCl solution with different concentrations of synthesized 4-chloro-1H-pyrazolo[3,4-d]pyrimidine (CHPP) was investigated by electrochemical measurements. CHPP has significantly inhibited mild steel corrosion in 1 M HCl solution and the inhibition efficiency increased with CHPP concentration. The inhibitor showed more than 87% inhibition efficiency at optimum concentration of 10^{-3} mol L⁻¹. Potentiodynamic polarization results showed that CHPP was a mixed-type inhibitor with predominately anodic effect. The adsorption of CHPP on mild steel surface was strong and followed Langmuir adsorption isotherm. The relationship between molecular structure of this compound and their inhibition efficiency has been investigated by quantum chemical calculations. The electronic properties such as the highest occupied molecular orbital (HOMO), the lowest unoccupied molecular orbital (LUMO) energy levels, energy gap (LUMO/HOMO), dipole moment and molecular orbital densities were computed.

1. Introduction

Mild steel has been widely used in industry as a material for reaction vessels, tunnels, etc... [1]. Acid solutions, especially hydrochloric acid, are usually employed for acid picking, acid cleaning, acid descaling and oil well acidizing, which may result in the corrosion of iron [2,3]. Damaged mild steel by aggressive media causes serious losses on the economy and potential problems in industrial equipment safety [4]. An effective method to protect metal from corrosion is the use of inhibitors. Currently, the corrosion behavior of material and the adsorption mechanism of organic inhibitors make great challenges [5–7]. Many compounds which contain hetero-atoms and multiple bonds are known as efficient corrosion inhibitors [8–11].

N-heterocyclic compounds are well qualified to play more protection for steel corrosion [12-14]. Many N-heterocyclic compounds such as derivatives of pyrazole [15-17], bipyrazole [18-20], triazole [21-23], tetrazole [24-26], imidazole [27-30], pyridine [31-34], pyrimidine [35], pyridazine [36,37] have been reported as effective corrosion inhibitors for steel in acidic media. The heterocyclic compound containing nitrogen atoms can easily be protonated in acidic medium to exhibit good inhibitory action on the corrosion of metals in acid solutions.

The purpose of this work is thus to investigate the corrosion inhibition of mild steel in 1 M HCl environment by the new synthesized 4-chloro-1H-pyrazolo[3,4-d]pyrimidine (CHPP) successively by means of weight loss, potentiodynamic polarization and (EIS) methods. The effect of temperature on the inhibitive properties of CHPP has been studied. Optical Microscopy (OM) has been applied. Quantum chemical calculations have been employed to explore the relationship between the molecular structures and the inhibition performance. The chemical structure of the studied (CHPP) derivative is given in scheme 1.



Scheme1: 4-chloro-1H-pyrazolo[3,4-d]pyrimidine (CHPP).

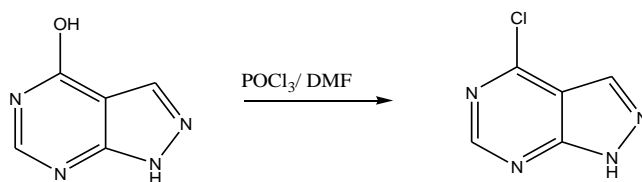
2. Experimental details

2.1. Materials and sample preparation

Mild steel was used for this study has the following composition; Mild Steel strips containing: 0.09 % P; 0.38 % Si; 0.01 % Al; 0.05 % Mn; 0.21 % C; 0.05 % S and the remainder iron. The specimen was used for electrochemical measurements; the exposed surface area was 1cm². The aggressive solutions of 1 M HCl were prepared by dilution of an analytical grade 37% HCl with double distilled water. The concentration range of inhibitor employed was 10⁻⁶ – 10⁻³(mol/L).

2.2.Synthesis of 4-chloro-1H-pyrazolo[3,4-d]pyrimidine

Chloration: 3 mmol of the 1H-pyrazolo[3,4-d]pyrimidin-4-one are heated at reflux in 3 ml of POCl₃ and 10 mL of DMF for 30 min. The reaction mixture is poured slowly on ice with agitation. The product precipitate is filtered; the obtained product was characterized by ¹H NMR, ¹³C NMR and mass.



Scheme 2:Chloration of allopurinol (CHPP).

The compound was characterised by NMR and mass. ¹H-NMR (DMSO-d₆) (d ppm): 8.01(s, 1H, C-H), 8.34 (s, 1H, C-H), 13.10 (s, 1H, N₁H).

¹³C-NMR (DMSO-d₆) (dppm): =CH, 136.95, 150.21, Cq: 110.10, 153.39, 153.69, HRMS (ESI) [M +H]: m/z = 155.07.

2.3. Corrosion monitoring methods

Potentiodynamic polarization was carried out in a conventional three-electrode electrolytic cell. Saturated calomel electrode (SCE) and platinum electrode were used as reference and auxiliary electrodes respectively. The working electrode made from mild steel having a surface of 1 cm² is in a rectangular form. These electrodes are connected to Volta lab PGZ 301 piloted by ordinate associated to “Volta Master 4” software. The scan rate was 1mV/s started from an initial potential of -800 to 0 mV/SCE. Before recording each curve, a stabilization time of 30 min was allowed.

Electrochemical impedance spectroscopy (EIS) was carried out with the same equipment used for the polarization measurements; sine wave voltage 10 mv peak to peak, at frequencies between 100 kHz and 10 mHz was superimposed on the rest potential. The impedance diagrams are given in the Nyquist representation. Experiments have been repeated three times to ensure there reproducibility.

2.4. Morphology of the steel surface

Immersion corrosion analysis of mild steel specimen in the acidic solutions with and without inhibitor was carried out using Optical microscopy (OM). After the corrosion tests, the samples were submitted to OM studies to know the surface morphology.

2.5. Quantum Chemical Calculations:

The Gaussian 09W software was used to do the Quantum chemical calculation. The B3LYP functional with 6311++G (d,p) basis set was used to geometrically optimized the molecular structure of 4-chloro-1H-pyrazolo[3,4-d]pyrimidine (CHPP) by density functional theory (DFT). The energy of lowest unoccupied molecular orbital (E_{LUMO}), the energy of highest occupied molecular orbital (E_{HOMO}), energy gap ($\Delta E = E_{LUMO} - E_{HOMO}$), and dipole moment (μ) were obtained from Quantum chemical calculation

3. Results and Discussion

3.1. Potentiodynamic Polarization Curves

The potentiodynamic polarization curves for mild steel in 1 M HCl solution in the absence and presence of different concentrations of this inhibitor are shown in Fig.1 at 303 K. It is apparent from the Fig. 1, that the nature of the polarization curves remains the same in the absence and presence of inhibitor but the curves shifted towards lower current density in the presence of inhibitor, indicating that the inhibitor molecules retard the corrosion process. The corrosion current densities and corrosion potentials were calculated by extrapolation of the linear parts of anodic and cathodic curves to the point of intersection.

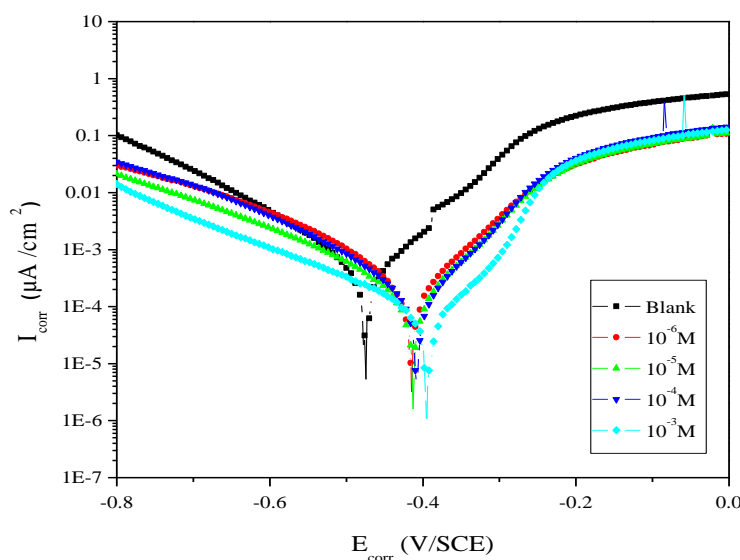


Figure1: Polarization curves of mild steel in 1 M HCl containing different concentrations of CHPP at 303K.

Electrochemical parameters such as corrosion current density (I_{corr}), corrosion potential (E_{corr}), anodic and cathodic Tafel slopes (β_a and β_c) were obtained from the intersection of anodic and cathodic Tafel lines and the inhibition efficiency ($\eta_{Tafel}\%$) were determined by Tafel extrapolation method and are given in Table 1. The efficiency (EI %) was calculated using equation (1) :

$$\eta_{Tafel}(\%) = \frac{I_{corr} - I_{corr(i)}}{I_{corr}} \times 100 \quad (1)$$

where I_{corr} and $I_{corr(i)}$ are the corrosion current densities in absence and presence of CHPP, respectively.

The results revealed that increasing the concentration of inhibitor leads to a decrease in corrosion current densities and an increase in inhibition efficiency ($\eta_{Tafel}\%$), suggesting the adsorption of inhibitor molecules at the surface of mild steel to form a protective film on the steel surface [10, 38]. Furthermore, both anodic (β_a) as well as cathodic Tafel (β_c) slopes for CHPP were observed to be change with increasing inhibitor concentration, resulting that the investigated inhibitors affect both reactions [39]. The presence of inhibitor causes a minor change in E_{corr} values with respect to the E_{corr} value in the absence of an inhibitor. This implies that the inhibitor act as a mixed-type inhibitor, affecting both anodic and cathodic reactions [40]. If the displacement in E_{corr} is more than ± 85 mV relating to the corrosion potential of the blank, the inhibitor can be considered as a cathodic or anodic type [41]. If the change in E_{corr} is less than ± 85 mV, the corrosion inhibitor may be regarded as a

mixed type. The maximum displacement in our study is 62 mV, which indicates that this inhibitor act as a mixed-type with predominately anodic effect.

Table1: Polarization parameters and the corresponding inhibition efficiency for the corrosion of mild steel in HCl1M containing different concentrations of CHPP at 303 K.

C (M)	$-E_{corr}$ (mV _{SCE})	β_a (mV dec ⁻¹)	$-\beta_c$ (mV dec ⁻¹)	I_{corr} (μ A cm ⁻²)	η_{Tafel} (%)
Blank	477	101	138	579	—
10 ⁻⁶	417	81	96	136	76.4
10 ⁻⁵	416	80	108	100	82.7
10 ⁻⁴	411	72	83	89.9	84.4
10 ⁻³	397	62	162	71.6	87.6

3.2. Electrochemical impedance spectroscopy measurements

The impedance measurements were carried out at room temperature after 30 min of immersion in 1 M HCl solution in the absence and presence of different concentrations of the CHPP inhibitor. The Nyquist plots for mild steel obtained at the interface in the presence and the absence of CHPP at different concentrations are given in Fig. 2. The charge-transfer resistance (R_{ct}) values are calculated from the difference in impedance at lower and higher frequencies as suggested by Tsuru et al [42]. The double layer capacitance (C_{dl}) and the frequency at which the imaginary component of the impedance is maximal ($-Z_{max}$) are found as represented in equation 2:

$$C_{dl} = \frac{1}{2\pi f_{max} R_{ct}} \quad (2)$$

The percentage IE% was calculated using the following equation and also given in table 2:

$$\eta_z (\%) = \left(1 - \frac{R_{ct}^{\circ}}{R_{ct}} \right) \times 100 \quad (3)$$

Where R_{ct} and R_{ct}° are charge transfer resistance with and without addition of CHPP respectively.

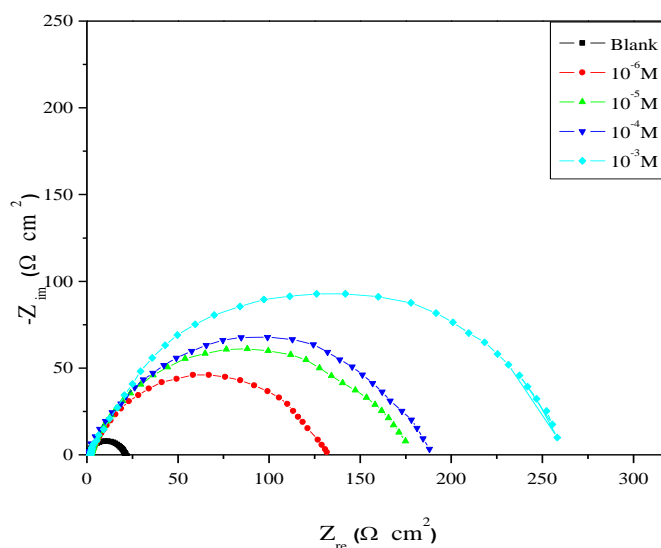


Figure 2: Nyquist plots for mild steel in 1 M HCl solution without and with different concentration of CHPP.

From table 2, it is obvious that the values of R_{ct} increases and the values of C_{dl} decreased with adding (CHPP) concentrations and this in turn leads to an increase in $\eta_z(\%)$. These results clearly indicate that the corrosion of mild steel in 1 M HCl solution is controlled by a charge transfer process [43]. The decrease of C_{dl} value

suggested that the inhibition can be attributed to the decrease in local dielectric constant and/or an increase in thickness of electrical double layer which resulted from the CHPP molecules adsorption at the mild steel surface/solution interface [44].

Table 2: Electrochemical Impedance for corrosion of steel in acid medium at various concentrations of CHPP.

C (M)	R _{ct} (Ω cm ²)	C _{dl} (μF/cm ²)	η _Z (%)
Blank	20.5	122.8	—
10 ⁻⁶	122	31.0	83.2
10 ⁻⁵	176	23.0	88.4
10 ⁻⁴	214	11.1	90.4
10 ⁻³	280	8.1	92.7

It is clear that, the corrosion of mild steel in 1 M HCl is clearly inhibited in the presence of the inhibitor, and the impedance response change with the increase in inhibitor concentration. Equivalent circuit as depicted in Figure.3 describes the metal/electrolyte interface of the present corroding system was used to simulate the impedance data in Fig.3.

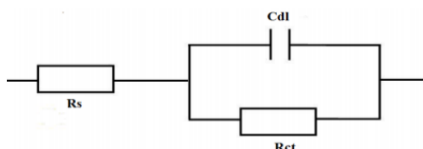


Figure 3: The standard Randle circuit

From the Table 2, the maximum percentage of inhibition efficiency η_Z(%) was achieved at the concentration of 10⁻³M (92.7%). In the presence of CHPP the values of R_{ct} has enhanced and the values of double layer capacitance C_{dl} are also brought down to the maximum extent with the increasing of the inhibitor concentration. The decrease in C_{dl} shows that the adsorption of the inhibitor takes place on the metal surface in acidic solution; which can result from a decrease in local dielectric constant and/or an increase in the thickness of the electric double layer [45].

3.3. Adsorption isotherm

The adsorption isotherm helps us to provide the information on the interaction between the inhibitor molecule of CHPP and the metal surface. The degree of surface coverage (θ) for different concentrations of inhibitor was evaluated from polarization measurements. Attempts were made to fit θ values to various isotherms such as Temkin, Frumkin and Langmuir. The best fit was obtained with the Langmuir isotherm (Fig. 4). From this isotherm, θ is linked to concentration inhibitor by following equation (4) [46].

$$\frac{C_{inh}}{\theta} = \frac{1}{K_{ads}} + C_{inh} \quad (4)$$

where C_{inh} is the inhibitor concentration, K_{ads} is equivalent constant and θ is the surface coverage.

It was found that from Fig.4 (plot of C_{inh}/θ versus C_{inh}) gives straight line with slope near to 1, indicating that the adsorption of compound under consideration on mild steel/acidic solution interface obeys Langmuir's adsorption. The thermodynamic parameters for the corrosion of mild steel in 1 M HCl in the presence and absence of different concentrations of CHPP are given in the Table 3.

The free adsorption energy is calculated from the equilibrium adsorption constant:

$$K_{ads} = \frac{1}{55.55} \exp\left(\frac{-\Delta G_{ads}^{\circ}}{RT}\right) \quad (5)$$

Where 55.5 is the concentration of water in mol.L⁻¹, R is the universal gas constant in J mol⁻¹.K⁻¹, T is the thermodynamic temperature in K. The plot of C_{inh}/θ versus C_{inh} yields a straight line with a slope 1.14, suggesting that the adsorptions on mild steel surface has followed Langmuir adsorption isotherm in HCl 1M solution. The slope, equilibrium constant and regression coefficient are presented in Table 3.

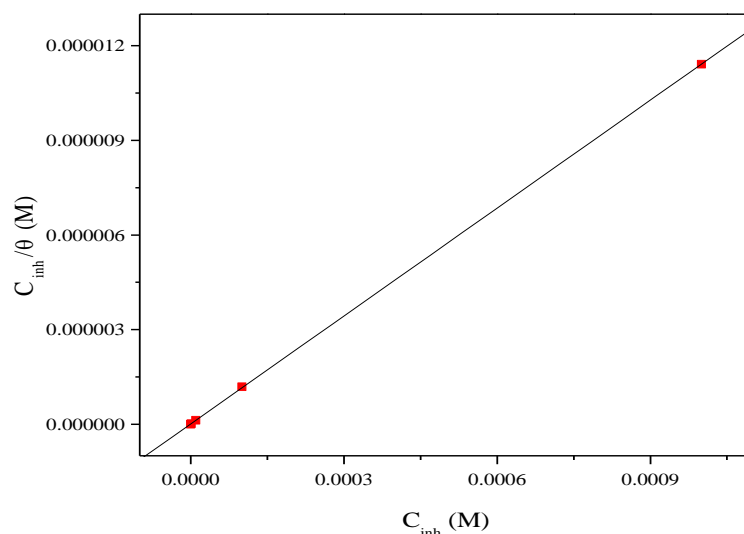


Figure 4: Langmuir adsorption plots for mild steel in 1 M HCl containing different concentrations of CHPP.

Table 3: Thermodynamic parameters for the corrosion of mild steel in 1 M HCl in the presence and absence of different concentrations of CHPP.

Inhibitor	R ²	Slope	K _{ads} (L/mol)	ΔG _{ads} ^o (kJ mol ⁻¹)
CHPP	0.9998	1.14	8.54×10 ⁵	-44.52

In the literature [47-49], if the absolute value of ΔG_{ads}^o is close to 20 kJ / mol or lower, the adsorption of the inhibitor is of the physical type, this type of adsorption is linked to electrostatic interactions Between the charged inhibitor molecules and the charged metal, whereas those close to 40 kJ / mol or higher imply a transfer of charges between the inhibitors (organic molecules) and the metal surface it is the chemisorption. Nonetheless, it is complicated to differentiate between chemisorption and physisorption only based on these criteria, especially when charged species are adsorbed. The possibility of Coulomb interactions between adsorbed cations and specifically adsorbed anions can increase the Gibbs energy even if no chemical bond appears [50]. The calculated ΔG_{ads}^o value for CHPP is -44.52 kJ mol⁻¹, indicating that the chemisorption mode is likely to predominate [51,52].

3.4. Effect of temperature

To investigate the nature of adsorption of the inhibitor and to calculate the activation energies of the corrosion process, polarisation measurements were obtained at different temperatures in the absence and the presence of CHPP and precisely in the range of temperature 303-333 K. Figs 5 and 6 give the polarization curves for mild steel in the absence and presence of 10⁻³M of CHPP at different temperatures. The corresponding data are given in Table 4.

Temperature is a factor that plays a significant role in the corrosion of a given material in a corrosive environment. The behavior of the former might be affected by temperature in addition to the possible modification in the metal-inhibitor interaction. It should be noted, however, that the temperature effect on the acid-metal inhibition reaction might be quite complex owing to the various changes occurring on the metal surfaces. For instance, rapid etching, inhibitor desorption and possible inhibitor decomposition [35,53].

The relationship between the density corrosion (I_{corr}) of mild steel in acidic media and temperature T is often expressed by the Arrhenius equation (6)[54].

$$I_{corr} = A \exp\left(\frac{-E_a}{RT}\right) \quad (6)$$

E_a is the activation energy of the corrosion process, A is the Arrhenius constant, R the general gas constant.

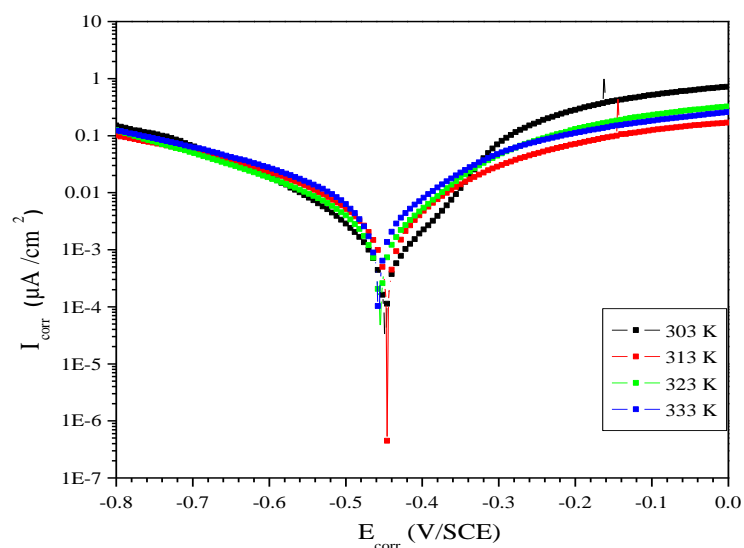


Figure 5: Polarization curve for mild steel in 1 M HCl at different temperatures.

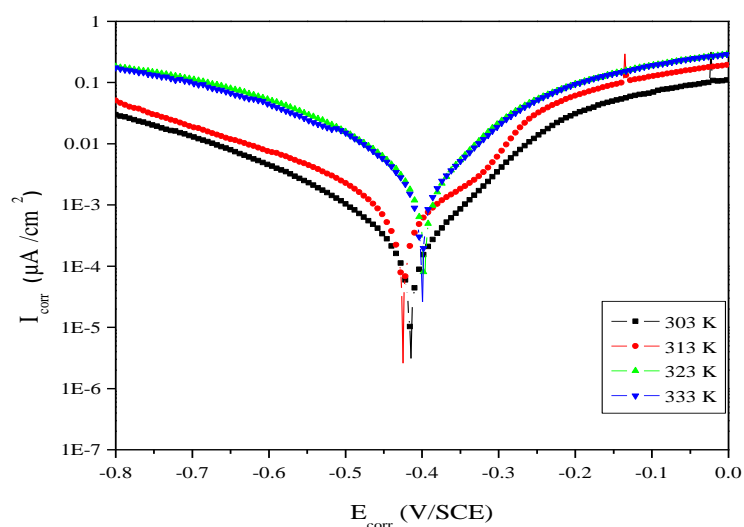


Figure 6: Polarization curve for mild steel in 1 M HCl + 10^{-3} M of CHPP at different temperatures.

The Experimental corrosion rate values obtained from polarization curves for mild in HCl1M in the absence and presence of CHPP was used to further gain insight on the change of enthalpy (ΔH_a) and entropy (ΔS_a) of activation for the formation of the activation complex in the transition state using transition equation [55]:

$$I_{corr} = \frac{RT}{Nh} \exp\left(\frac{\Delta S_a}{R}\right) \exp\left(-\frac{\Delta H_a}{RT}\right) \quad (7)$$

Where h is the planks constant, N is Avogadro's number, ΔS_a is the apparent entropy of activation and ΔH_a is the apparent enthalpy of activation.

The values of E_a , ΔH_a and ΔS_a were estimated from the slopes of the straight lines and given in Table 5. The plot of $\ln(I_{corr})$ against $1/T$ and $\ln(I_{corr}/T)$ versus $1/T$ for mild steel in 1 M HCl in the absence and presence of different concentrations of CHPP are presented in Figure 7 and Figure 8. All parameters are given in Table 5. In the present study, it could be seen that the activation energy was higher in the presence of CHPP when compared with the blank. Furthermore, with increasing concentration of CHPP, the activation energy increased. The increase in activation energies in the presence of inhibitor is attributed to an appreciable decrease in the adsorption process of the inhibitor on the metal surface with increase in temperature; and corresponding increase in the reaction rate because of the greater area of the metal exposed to acid [8,10,53].

Table 4: Thermodynamic parameters for the adsorption of CHPP on the mild steel at different temperatures

T (K)	C (M)	-E _{corr} (mV _{SCE})	I _{corr} (μA cm ⁻²)	η _{Tafel} (%)
303	Blank	477	579	—
	CHPP	397	71.6	87.6
313	Blank	448	716.1	—
	CHPP	426	163.8	77.1
323	Blank	457	2073	—
	CHPP	399	696.6	66.3
333	Blank	458	2076	—
	CHPP	404	704.2	66.0

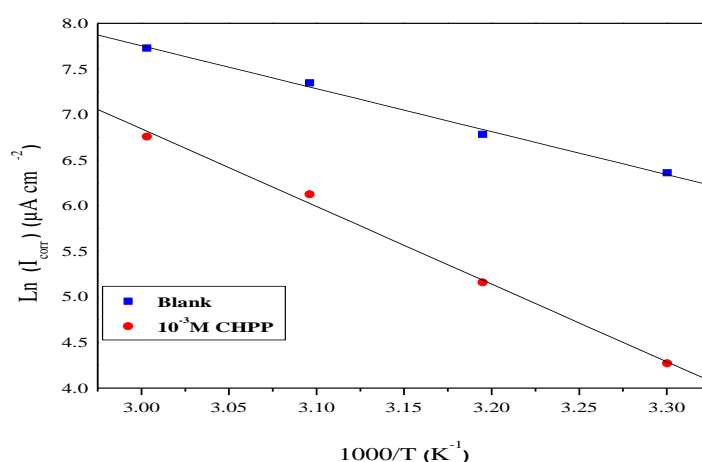


Figure 7: Arrhenius plots of Ln I_{corr} vs. 1/T for steel in 1 M HCl in the absence and the presence of CHPP at optimum concentration

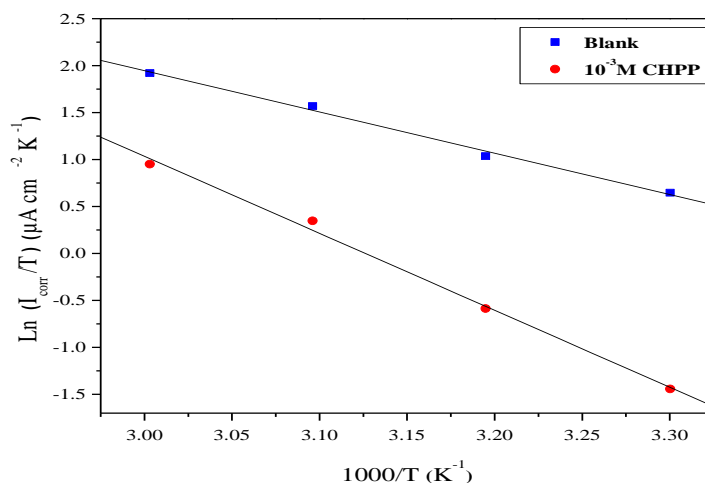


Figure 8: Transition Arrhenius plots of mild steel in 1 M HCl with and without 10⁻³M of CHPP.

Table 5: Activation parameters for the steel dissolution in 1 M HCl in the absence and the presence of CHPP at optimum concentration.

Medium	R ²	E _a (kJ mol ⁻¹)	ΔH _a (kJ mol ⁻¹)	ΔS _a (J mol ⁻¹ K ⁻¹)
Blank	0.9998	40.32	37.04	-70.13
CHPP	0.9997	70.14	67.70	14.21

Inspection of table 5 data revealed that the thermodynamic ΔH_a and ΔS_a parameters for dissolution reaction of mild steel in 1 M HCl in the presence of inhibitor is higher ($37.04 \text{ kJ mol}^{-1}$ and $-70.13 \text{ J mol}^{-1} \text{ K}^{-1}$) than that of in the absence of inhibitor, ($67.70 \text{ kJ mol}^{-1}$ and $14.21 \text{ J mol}^{-1} \text{ K}^{-1}$) respectively. The positive sign of ΔH_a reflect the endothermic nature of the steel dissolution process suggesting that the dissolution of steel is slow [56] in the presence of inhibitor. The negative value of ΔS_a for mild steel in 1 M HCl implies that the activated complex is the rate-determining step, rather than the dissociation step. In the presence of the inhibitor, the value of ΔS_a increases and is generally interpreted as an increase in disorder as the reactants are converted to the activated complexes [57].

3.5. Optical microscopy measurements

The surface morphology of mild steel was showed by optical microscopy after 24 hours immersion in 1 M HCl before and after addition of the inhibitor. Fig. 9 (a) give the obtained micrograph of polished steel without being exposed to the corrosive solution, while Fig. 9(b) illustrates a strongly damaged steel surface due to the formation of corrosion products after immersion in 1 M HCl solution. OM images of mild steel surface after immersion in 1 M HCl with 10^{-3} M of CHPP is shown in Fig. 9(c).

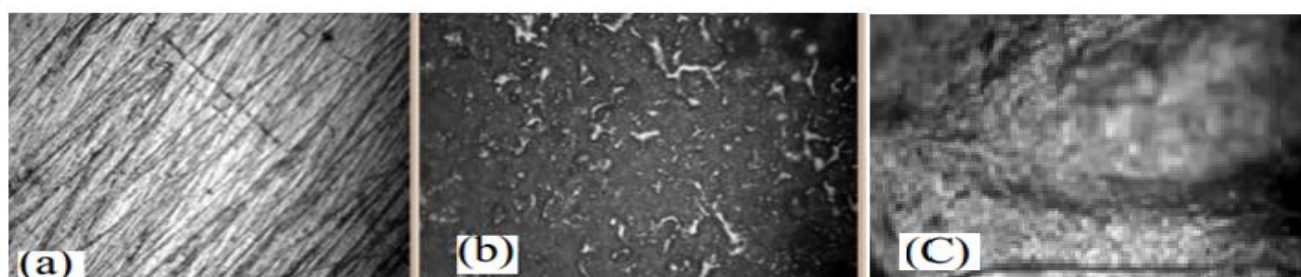


Figure 9: OM (x50) of CHPP (a) before immersion (b) after 24 hours of immersion in 1 M HCl (C) after 24 hours of immersion in 1 M HCl + 10^{-3} M CHPP at 303 K.

It can be seen from Fig.9a that the mild steel sample before immersion seems smooth and shows some abrading scratches on the surface. An aggressive attack of the corroding medium on the mild steel surface was shown in Figure.9b after immersion in uninhibited 1 M HCl. However, in the presence of 10^{-3} M of CHPP (Fig. 9c), the mild steel surface was tightly corroded. Moreover, an adsorbed layer on the steel surface was created and that was not observed in Fig.9b. The result was a strengthening the surface coverage on the steel surface thus it reduces the contact between the steel and the aggressive medium. Consequently, a good protective film was formed can efficiently inhibit the corrosion of steel.

3.6. Quantum chemical calculations

Quantum chemical calculations have been conducted in order to understand inhibition mechanism of CHPP for mild steel in corrosion media at 303 K. Especially, optimized geometric structures, Electrostatic surface potential and frontier molecular orbital of CHPP including the electron density distributions of HOMO and LUMO for CHPP were shown as Fig. 10.

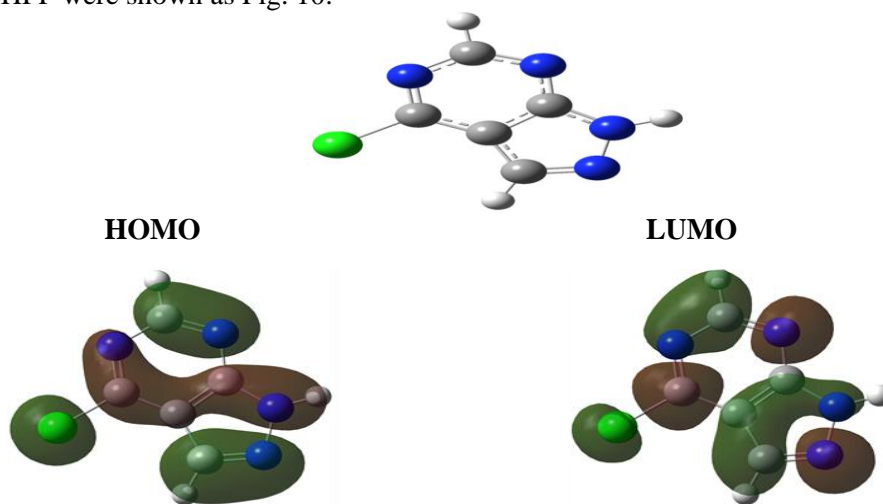


Figure10: Optimized structure and frontier molecular orbital of CHPP.

Then, the parameters about quantum chemical calculation were showed in Table 7. There are not only including the energy of the highest occupied molecular orbital (E_{HOMO}) but also containing the lowest unoccupied molecular orbital (E_{LUMO}) of the inhibitor molecular. Besides the energy gap ($\Delta E = E_{\text{LUMO}} - E_{\text{HOMO}}$) and dipole moment (μ) are analyzed.

Table 7: The parameters about Quantum chemical calculation.

Quantum Parameters	CHPP
E_{HOMO} (eV)	-7.59703909
E_{LUMO} (eV)	-2.29198253
μ (debye)	1.55
ΔE (gap) (eV)	5.30505656

The value of highest occupied molecular orbital, E_{HOMO} indicates the tendency of the molecule to donate electrons through nitrogen atoms to acceptor molecule with empty and low energy orbital. E_{LUMO} indicates the tendency of the molecule to accept electrons, with the trend often being that the lower E_{LUMO} is, the greater is the ability of that molecule to accept electrons [58]. The energy gap ΔE is an important parameter that is related to reactivity of the inhibitor molecule towards the metal surface. A high ΔE is associated with a less tendency towards reactivity while a low ΔE is an indication of a great tendency towards reactivity [59]. Polarity of a covalent bond (Dipole moment μ) can be understood by distribution of electrons in a molecule and large values of dipole moment μ favour the adsorption of inhibitor.

Conclusion

The 4-chloro-1H-pyrazolo [3,4-d]pyrimidine(CHPP) was found to be a good inhibitor for the corrosion of mild steel in 1 M HCl solution. Inhibition efficiency increases with increase in CHPP concentration, but decrease with increase in temperature. Double-layer capacitances decrease with respect to blank solution when the synthesized inhibitor is added. This fact can be explained by adsorption of the synthesized inhibitor species on the mild steel surface. Polarization studies reveal that CHPP act as a mixed-type inhibitor with predominately anodic effect. The adsorption of CHPP on mild steel surface can be approximated by Langmuir isotherm model.

References

1. Migahed M.A., Abdul-Raheim A.M., Atta A.M., Brostow W., *Mater. Chem. Phys.* 121 (2010) 214.
2. Singh D.D.N., Singh T.B., Gaur B., *Corros. Sci.* 37 (1995) 1019.
3. Badr G.E., *Corros. Sci.* 51 (2009) 2536.
4. Asefi D., Arami M., Mahmoodi N.M., *Corros. Sci.* 52 (2010) 800.
5. El Adnani Z., Mcharfi M., Sfaira M., Benzakour M., Benjelloun A.T., EbnTouhami M., *Corros. Sci.* 68 (2013) 230.
6. Sam J., Abraham J., *Ind. Eng.Chem. Res.* 51 (2012) 1642. 7. Yongming T., Fan Z., Hu S., Ziyi C., Wu Z., Wenheng Jing, *Corros. Sci.* 74 (2013) 282.
8. Harmaoui A., Bourazmi H., El Fal M., Boudalia M., Tabyaoui M., Guenbour A., Bellaouchou A., Essassi E.M., *J. Mater. Environ. Sci.* 6 (2015) 2519.
9. Xu B., Yang W., Liu Y., Yin X., Gong W., Chen Y., *Corros. Sci.* 78 (2014) 268.
10. Chami R., Bensajay F., Alehyen S., El Achouri M., Boudalia M., Marrakchi K., Bellaouchou A., Genbour A., *J. Mater. Environ. Sci.* 8 (2017) 30
11. Wang L., Yin G.J., Yin J.G., *Corros. Sci.* 43 (2001) 1202.
12. Hammouti B., Zarrouk A., Al-Deyab S.S., Warad I., *Oriental J. Chem.* 27(2011) 23.
13. Foad El Sherbini E.E., *Mater. Chem. Phys.* 60 (1999) 286.
14. Frenier W.W., Growcock F.B., Lopp V.R., *Corrosion.* 44 (1988) 590.
15. Quraishi M.A., Jamal D., *Corrosion.* 56 (2000) 156.
16. Benabdellah M., Yahyi A., Dafali A., Aouniti A., Hammouti B., Ettouhami A., *Arab. J. Chem.* 4 (2011) 343.
17. Elayyachy M., Hammouti B., El Idrissi A., Aouniti A., *Port. Electrochim. Acta.* 29 (2011) 57.

18. Sykes J.M., *Br. Corros. J.* 25 (1990) 175.
19. Chatterjee P., Banerjee M.K., Mukherjee K.P., *Indian J. Technol* 29 (1991) 191.
20. Bockris JO'M., Yang B., *J. Electrochem. Soc.* 138 (1991) 2237.
21. Zarrouk A., Warad I., Hammouti B., Dafali A., Al-Deyab S.S., Benchat N., *Int. J. Electrochem. Sci.* 5 (2010) 1516.
22. Vermilyea DA., in, *First International Congress; Metal Corrosion; Butterworths; London; (1962)* 62
23. Bentiss F., Traisnel M., Chaibi N., Mernari B., Vezin H., Lagrenee M., *Corros. Sci.* 44 (2002) 2271.
24. El Ouali I., Hammouti B., Aouniti A., Ramli Y., Azougagh M., Essassi E.M., Bouachrine M., *J. Mater. Environ. Sci.* 1 (2010) 1.
25. Khaled K.F., Abdelshafi N.S., El-Maghraby A., Al-Mobarak N., *J. Mater. Environ. Sci.* 2 (2011) 166.
26. Uhrea J., Aramaki K., *J. Electrochem. Soc.* 138 (1991) 3245.
27. Kertit S., Hammouti B., *Appl. Surf. Sci.* 93 (1996) 59.
28. Chetouani A., Hammouti B., Aouniti A., Benchat N., Benhadda T., *Prog. Org. Coat.* 45 (2002) 373.
29. Bekkouch K., Aouniti A., Hammouti B., Kertit S., *J. Chim. Phys.* 96 (1999) 838.
30. Kertit S., Hammouti B., Taleb M., Brighli M., *Bull. Electrochem.* 13 (1997) 241.
31. Bouklah M., Benchat N., Aouniti A., Hammouti B., Benkaddour M., Lagrenee M., Vezin H., Bentiss F., *Prog. Org. Coat.* 51 (2004) 118.
32. Wang L., *Corros. Sci.*, 48 (2006) 608.
33. Lagrenee M., Mernari B., Chaibi N., Traisnel M., Vezin H., Bentiss F., *Corros. Sci.* 43 (2001) 951.
34. Rengamani S., Muralidharan S., AnbuKulandainathan M., VenkatakrishnaIyer S., *J. Electrochem. Soc.* 24 (1994) 355.
35. Boudalia M., Bellaouchou A., Guenbour A., Bourazmi H., Tabiyaoui M., El Fal M., Ramli Y., Essassi E M., Elmsellem H., Hammouti B., *Mor. J. Chem.* 2 (2014) 109
36. Zarrok H., Saddik R., Oudda H., Hammouti B., El Midaoui A., Zarrouk A., Benchat N., EbnTouhami M., *Der Pharma Chemica.* 3 (2011) 272
37. Chetouani A., Hammouti B., Aouniti A., Benchat N., Benhadda T., *Prog. Org. Coat.* 45 (2003) 73.
38. Wang X., Yang H., Wang F., *Corros. Sci.* 53 (2011) 113.
39. Jayaperumal D., *Mater. Chem. Phys.* 119 (2010) 478.
40. Ferreira E. S., Giancomlli C., Giacomlli F. C., Spinelli A., *Mater. Chem. Phys.* 2004
41. Suru T., Haruyama T., Gijutsu S., *B.J. Jpn. Soc. Corros. Eng.* 27 (1978) 573
42. Ramesh S., Rajeswari S., *Electrochim. Acta* 49(2004) 811.
43. Ashassi-Sorkhabi H., Shaabani B., Seifzadeh D., *App. Surf. Sci.* 239 (2005) 154.
44. McCafferty E., Hackerman N., *J. Electrochem Soc.* (1972) 119.
45. Do D., *Adsorption Analysis: Equilibria and Kinetics*, Imperial College Press (1980).
46. Kosec T., Milošev I., Pihlar B., *Appl. Surf. Sci.* 253 (2007) 8873.
47. Mehaute A. H., Greppe G., *Solid State Ionics* 9-10 (1983) 30.
48. Scendo M., *Corros. Sci.* 47 (2005) 2791.
49. Salim R., Ech Chihbi E., Oudda H., ELAoufir Y., El-Hajjaji F., Elaattiaoui A., Oussaid A., Hammouti B., Elmsellem H., Taleb M., *Der Pharma Chemica*, , 8(13) (2016) 200-213
50. De Costa S.L., Agostinho S. M. L., Nobe K., *J. Electrochem. Soc.* 140 (1993) 3488.
51. Zhao T. P., Mu G. N., *Corros. Sci.* 41 (1999) 1944.
52. Noor E. A., *Int. J. EElectrochem. Sci.* 2 (2007) 1017.
53. Abboud Y., Abourriche A., Saffaj T., Berrada M., Charrouf M., Bennamara A., Hannache H., *Desalination* 237(2009) 175.
54. Obot I.B., Obi-Egbedi N.O., *Corros. Sci.* 52 (2010) 204.
55. Martinez S., Stern I., *Appl. Surf. Sci.* 199 (2002) 83.
56. Hosseini S.M.A., Salari M., Ghasemi M., Abaszadeh M., *Z. Phys. Chem.*, 223 (2009) 769.
57. Xia S., Qiu M., Yu L., Liu F., Zhao H., *Corros. Sci.* 50 (2008) 2021.
58. Ebenso E.E., Arslan T., Kandemirli F., Caner N., Love I., *Int. J. Quant. Chem.* 110 (2010) 1003.
59. Li X., Deng S., Fu H., Li T., *Electrochim. Acta* 54 (2009) 4089

(2017) ; <http://www.jmaterenvirosnci.com>